

# Seer: Language Instructed Video Prediction with Latent Diffusion Models

Xianfan Gu<sup>1</sup> Chuan Wen<sup>1,2,3</sup>

<sup>1</sup>Shanghai Qi Zhi Institute

<sup>3</sup>Shanghai Artificial Intelligence Laboratory

Jiaming Song<sup>4</sup> Yang Gao<sup>1,2,3</sup>

<sup>2</sup>IIIS, Tsinghua University

<sup>4</sup>NVIDIA

## Abstract

*Imagining the future trajectory is the key for robots to make sound planning and successfully reach their goals. Therefore, text-conditioned video prediction (TVP) is an essential task to facilitate general robot policy learning, i.e., predicting future video frames with a given language instruction and reference frames. It is a highly challenging task to ground task-level goals specified by instructions and high-fidelity frames together, requiring large-scale data and computation. To tackle this task and empower robots with the ability to foresee the future, we propose a sample and computation-efficient model, named **Seer**, by inflating the pretrained text-to-image (T2I) stable diffusion models along the temporal axis. We inflate the denoising U-Net and language conditioning model with two novel techniques, Autoregressive Spatial-Temporal Attention and Frame Sequential Text Decomposer, to propagate the rich prior knowledge in the pretrained T2I models across the frames. With the well-designed architecture, Seer makes it possible to generate high-fidelity, coherent, and instruction-aligned video frames by fine-tuning a few layers on a small amount of data. The experimental results on Something Something V2 (SSv2) and Bridgedata datasets demonstrate our superior video prediction performance with around 210-hour training on 4 RTX 3090 GPUs: decreasing the FVD of the current SOTA model from 290 to 200 on SSv2 and achieving at least 70% preference in the human evaluation.*

## 1. Introduction

Enabling robots to follow human instructions and complete complex tasks in real environments is the vision for the next generation of robotics learning. However, the instructions are often highly abstract outlines of task goals that require long-horizon operations of the robot to complete. As a result, learning a mapping between abstract language instructions and specific policy actions at each time step presents a significant challenge. In contrast, humans employ an imagining-planning approach: when presented with a text instruction for a particular task, e.g., “spinning cube

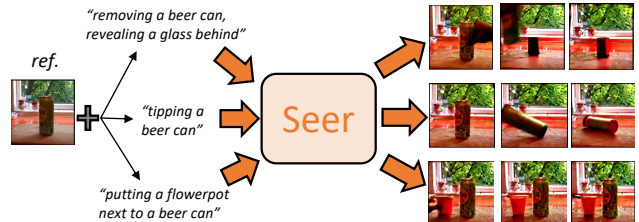


Figure 1: Seer is an efficient video diffusion model that uses natural language instructions and reference frames (ref.) to predict multiple variations of future frames.

that quickly stops spinning”, they can imagine the future trajectories in their minds and plan accordingly. Therefore, generating videos conditioned on a few frames and language instructions, i.e., text-conditioned video prediction (**TVP**), is a fundamental task for robots to perform complex and long-horizon control and manipulation tasks. By training large models on large-scale datasets, TVP can address the insufficient training data problem in robotics and facilitate the development of general robot policy learning.

Despite its potential benefits, text-conditioned video prediction (TVP) is a challenging task because it requires a deep understanding of the initial frames, the natural language instruction, and the grounding between language and images, while predicting based upon all the information above. The traditional text-conditioned video generation task [35, 36, 13, 12, 26] does not condition on initial frames and thus a model could seemingly perform well if it only generates a few prototypical videos corresponding to the input text. The TVP task is much more challenging as the initial frames are given and generating prototypical videos is no longer a solution. Besides, the existing text-conditioned video generation task usually aims to generate short horizon video clips with text specifying the general content, such as “a person is skiing”, while our aim in the TVP task is to use the text as a “task descriptor” in robotics, such as “tipping a beer can”, as shown in Figure 1.

Specifically, there are mainly three problems limiting the performance of the TVP task: **1) Requirement for large-scale labeled text-video datasets and expensive computation**

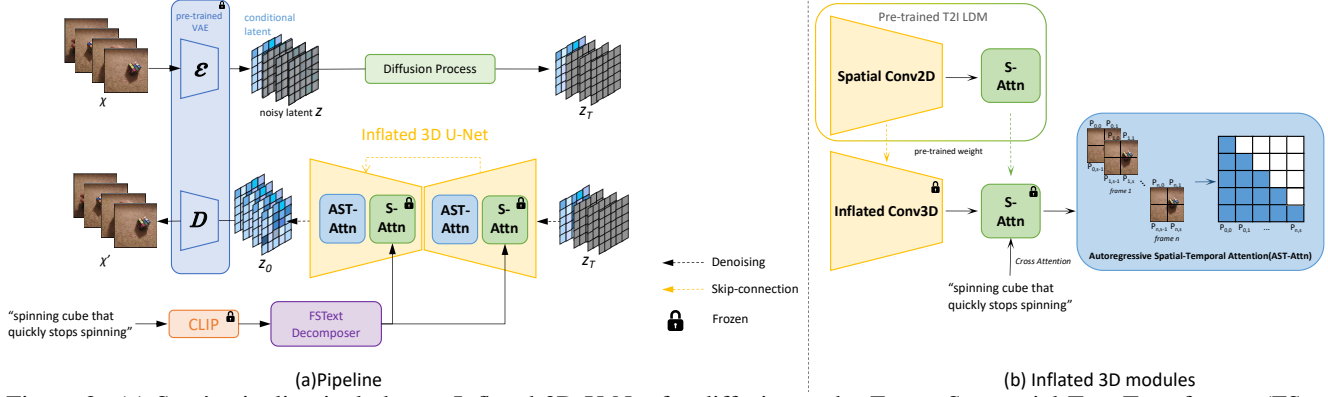


Figure 2: (a) Seer’s pipeline includes an Inflated 3D U-Net for diffusion and a Frame Sequential Text Transformer (FSeq Text Transformer) for text conditioning. During training, all video frames are compressed to latent space with a pre-trained VAE encoder. Conditional latent vectors, sampled from reference video frames, are concatenated with noisy latent vectors along the frame axis to form the input latent. During inference, the conditional latent vectors are concatenated with Gaussian noise vectors, and the denoised outputs are decoded to RGB video frames with the pre-trained VAE decoder. (b) Our Inflated 3D U-Net expands the 2D Conv kernel of a pre-trained T2I latent diffusion model (LDM) to 3D kernels and connects the cross-attention layer with the Autoregressive Spatial-Temporal Attention (AST-Attn) layer.

**tational cost:** learning to capture the correspondence between two different modalities is non-trivial and needs large amounts of supervised text-video pairs and excessive computation overhead for training. **2) Low fidelity of generated frames:** the frames generated by the models are usually blurry and cannot clearly display the background and objects specified in the reference frames. **3) Lack of fine-grained instruction for each frame in the task-level videos:** the goals specified by text instructions are usually in the task level, making it difficult to understand the progress and generate the corresponding frame in each timestep only conditioned on a global text embedding. To address these issues, we propose **Seer**: a TVP method capable of generating task-level videos according to the text guidance with high data and training efficiency.

Motivated by the recent progress on generative models [22, 19], we propose to leverage text-to-image (T2I) latent diffusion models [22] for the TVP tasks. T2I models are pretrained with billions of text-image pairs crawled from the internet [25]. They have acquired rich prior knowledge and thus are able to generate high-quality images corresponding to the text descriptions. Therefore, inheriting such prior knowledge by inflating a T2I model along the temporal axis and fine-tuning it with a small text-video dataset is an appealing solution for TVP tasks, which relieves the requirement for extensive labeled data and computational overhead, i.e., Problem 1.

Since the T2I models contain two modalities: image and language, we propose to inflate these two parts to generate high-quality video frames and fine-grained text instruction embeddings for each timestep respectively. For the visual model, we extend the 2D latent diffusion model by insert-

ing an **Autoregressive Spatial-Temporal Attention** (AST-Attn) layer into the denoising U-Net [22] to model spatial dependencies and the temporal dynamics simultaneously, which is called Inflated 3D U-Net. By taking advantage of joint modeling of spatial and temporal dimensions, as well as autoregressive generation, we successfully synthesize coherent and high-fidelity frames, which alleviates Problem 2. As for the language module, in contrast to existing approaches [42, 37] that encode one text embedding for the whole video with a text encoder, we propose to decompose the single text instruction into fine-grained guidance embeddings for each time step. We achieve the automatic decomposition by a **Frame Sequential Text** (FSText) Decomposer based on the causal attention mechanism. By temporally splitting the instruction into different phases, Seer improves the guidance embeddings for each frame and thus enables the generation of task-level videos (Problem 3).

We conduct extensive experiments on Something-Something V2 [6] and Bridge Data [3] datasets. We outperform all the baselines, such as TATS [5], MCVD [34] and *Tune-A-Video* (TAV) [37], and achieve state-of-the-art video prediction performance in terms of FVD and KVD. Especially we improve FVD from 291 to 200, and KVD from 0.91 to 0.30 on Something-Something V2, compared to the SOTA TAV. Compare to over 480 hours with  $13 \times 8$  A100 GPUs in CogVideo [13], the experiments show the high efficiency of our method: 214 hours with 4 RTX 3090 GPUs. The ablation studies illustrate the effectiveness of our two technical contributions: AST-Attn and FSText Decomposer. Furthermore, our method supports video manipulation by modifying the text instructions, and we demonstrate our superior generation quality through a human evaluation study,

showing more than 70% preference for us over TAV and around 90% preference for us over TATS and MCVD.

## 2. Related Work

### 2.1. Text-to-Image Generation

Since Scott Reed et al. [21] firstly set up the T2I generation task and proposed a GAN-based method, this multi-modal generation task has attracted the attention of the computer vision community. DALL-E [20] makes a breakthrough by modeling the T2I generation task as a sequence-to-sequence translation task with a VQ-VAE [32] and Transformer [33]. Since then, many variants have been proposed with an improved image tokenizer [39], hierarchical Transformers [2] or domain-specific knowledge [4]. With the recent progress of Denoising Diffusion Probabilistic Models (DDPM) [10], the diffusion models have been widely used for T2I generation tasks [17, 23, 19, 7]. Specifically, GLIDE [17] proposes classifier-free guidance for T2I diffusion models to improve image quality. For a better alignment between text and image, DALL-E 2 [19] proposed to denoise CLIP [18] image embedding conditioned on CLIP text embedding, which integrated high-level semantic information. To reduce the computation cost of the denoising process in pixel space, Latent Diffusion Model (LDM) employs VAE [16] to operate in the latent space. Seer takes advantage of the prior language-vision knowledge of pretrained LDM and inflates it along the time axis.

### 2.2. Text-to-Video Generation

In contrast to the huge success of Text-to-Image (T2I) generation, Text-to-Video (T2V) generation is still under-explored due to the limitation of the large text-video data annotation and computing resources. Inspired by the various variants of T2I generation, recent T2V studies have attempted to explore compatible variants for video generation modeling. GODIVA [35] first proposes a VQ-VAE based auto-regressive model with three-dimensional sparse attention for T2V generation. NÜWA [36] further improves it by designing a 3D encoder with 3D nearby attention and achieves competitive performance on multi-task generation. Unlike the single frame-rate T2V approaches trained from scratch on large-scale text-video datasets, CogVideo [13] proposes a multi-frame-rate hierarchical model for T2V generation. This approach leverages the pre-trained module of T2I CogView-2 [2].

Motivated by the remarkable progress of T2I diffusion models [19, 23, 22], Make-A-Video [26], MagicVideo [43], Tune-A-Video [37] and Imagen Video [9] transfer the 2D diffusion models to 3D models by incorporating temporal modules in T2V generation. In contrast to Imagen Video, all other three methods utilize the prior knowledge of T2I pre-trained model. Similarly, we use the pre-trained weight

of the 2D T2I diffusion model in our 3D T2V model. Varying from the aforementioned methods, our method Seer utilizes autoregressive attention on both spatial and temporal spaces to generate high-fidelity and coherent video frames. And Seer is able to handle the task-level video prediction by decomposing the language condition into fine-grained sub-instruction embeddings.

## 3. Preliminaries

**Denoising Diffusion Probabilistic Models with classifier-free guidance:** Diffusion models are probabilistic models that approximate the data distribution by iteratively adding noise and denoising through a forward/reverse Gaussian Diffusion Process [10, 28]. The forward process applies noise at each time step  $t \in 0, \dots, T$  to the data distribution  $\mathbf{x}_0$ , creating a noisy sample  $\mathbf{x}_t$  where  $\mathbf{x}_t = \sqrt{\bar{\alpha}_t} \mathbf{x}_0 + \sqrt{1 - \bar{\alpha}_t} \epsilon$  ( $\epsilon \sim \mathcal{N}(\mathbf{0}, \mathbf{I})$ ), and  $\bar{\alpha}_t$  is the accumulation of the noise schedule  $\alpha_{0:T}$  defined by  $\bar{\alpha}_t = \prod_{s=1}^t \alpha_s$ . To denoise images, the diffusion process uses a reparameterized variant of Gaussian noise prediction  $\epsilon_\theta(\mathbf{x}_t, t)$  targeting Gaussian noise  $\epsilon$ . The reverse process  $p(\mathbf{x}_{t-1}|\mathbf{x}_t)$  of the Markov Chain generates new samples from Gaussian noise, which is approximated by Bayes' theorem as  $q(\mathbf{x}_{t-1}|\mathbf{x}_t, \mathbf{x}_0)$ , where  $\mathbf{x}_0$  is derived from the forward process as  $\mathbf{x}_0 = \frac{1}{\sqrt{\bar{\alpha}_t}}(\mathbf{x}_t - \sqrt{1 - \bar{\alpha}_t} \epsilon_\theta(\mathbf{x}_t, t))$ .

Classifier-free guidance [11] is introduced for conditional diffusion models to generate images without requiring an extra image classifier. A conditional model with a parameterized reverse process  $p(\mathbf{x}_{t-1}|\mathbf{x}_t, \mathbf{c})$  uses a conditional identifier  $\mathbf{c}$  through  $\epsilon_\theta(\mathbf{x}_t, t, \mathbf{c})$ . To predict an unconditional score, the conditional identifier is replaced with a null token  $\emptyset$  and denoted as  $\epsilon_\theta(\mathbf{x}_t, t, \mathbf{c} = \emptyset)$ . Classifier-free guidance can then be approximated as a linear combination of conditional and unconditional predictions:

$\tilde{\epsilon}_\theta(\mathbf{x}_t, t, \mathbf{c}) = (1+w)\epsilon_\theta(\mathbf{x}_t, t, \mathbf{c}) - w\epsilon_\theta(\mathbf{x}_t, t, \mathbf{c} = \emptyset)$ , (1)

where  $w$  is the guidance scale. Text-video and text-image-based diffusion models [22, 23, 17, 12, 26] use DDPM with classifier-free guidance. This diffusion framework can be adapted to various tasks with flexibility.

**Latent Diffusion Models:** Compared with image diffusion, video diffusion has significantly higher computation costs because it needs to process multiple frames. Recent works have explored the computation-efficient version of diffusion modeling, such as latent diffusion model (LDM) [22]. LDM proposes the VAE-based latent diffusion, including a KL-regularized autoencoder for encoding/decoding latent representation  $\epsilon(\mathbf{x})$ , and a diffusion model to operate on the latent space  $\mathbf{z}_t$ . For the conditional generation, LDM introduces a domain-specific encoder  $\tau_\theta$  to the projection of condition  $\mathbf{y}$  for various modality generations. Thus, the objective of LDM is:

$$L_{\text{LDM}} = \mathbb{E}_{t, \epsilon(\mathbf{x}), \mathbf{y}, \epsilon \sim \mathcal{N}(\mathbf{0}, \mathbf{I})} \left[ \|\epsilon - \epsilon_\theta(\mathbf{z}_t, t, \tau_\theta(\mathbf{y}))\|^2 \right] \quad (2)$$

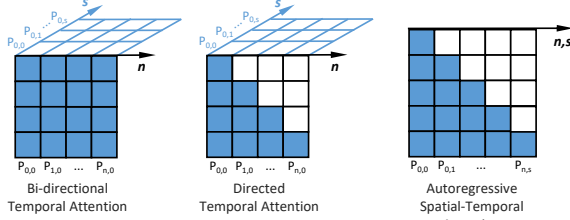


Figure 3: Variants of temporal attention layer, where  $P$  is the location of latent vectors relative to the axis of spatial space  $s$  and temporal space  $n$ .

## 4. Methodology

In this paper, we aim to explore an efficient diffusion method to predict coherent video frames guided by language instructions. However, it is challenging to directly apply conventional video diffusion models for TVP due to the following problems: (1) The limited labeled text-video data and computational resources. (2) Low fidelity of frame generation. (3) Lack of fine-grained instruction for each frame in the task-level videos.

Since our diffusion model is a 3D latent-based diffusion model, we address these problems by inflating the 2D latent diffusion model [22] along the temporal dimension. Specifically, we propose an inflated 3D U-Net to extend the prior knowledge contained in Stable Diffusion across the frames to generate high-quality and coherent frames (Sec. 4.1). To achieve this, we insert an Autoregressive Spatial-Temporal Attention layer (Sec. 4.2). As for the language conditioning model, we propose a Frame Sequential Text (FSText) Composer to adaptively decompose the text instruction into sub-conditions for each frame (Sec. 4.3).

### 4.1. Video Diffusion via Inflated Model

For the challenging TVP task, learning to parse natural language, understand the scene, and ground the language and scene together requires large-scale text-video datasets, which causes expensive computation and data annotation costs. With the development of conditional diffusion models, the text-to-image (T2I) models capture the underlying data distribution in large-scale datasets and thus get the capability to compose images with unseen objects specified by the text instructions. Motivated by this, we propose to take advantage of the prior knowledge implied in pretrained T2I models by inflating the T2I pre-trained latent diffusion model (LDMs) along the temporal axis, which will significantly reduce the need for large-scale training samples.

Since the T2I latent diffusion models consist of two main components: the image diffusion module and the language conditioning module [22]. We propose to inflate these two parts to perform the synthesis of high-fidelity frames and the temporal decomposition of text instructions, respectively.

Specifically, as shown in Figure 2 (a), we propose an Inflated 3D U-Net with the autoregressive spatial-temporal attention (AST-Attn) technique for the frame generation module in Section 4.2, and a Frame Sequential Text (FSText) Composer for text conditioning module in Section 4.3. Overall, we adopt two pathways to implement the conditional diffusion process of language guidance and reference frames. During training, we stack the latent space of the reference frames with the noisy latent space of the remaining frames along the temporal dimension. During inference, we predict future frames by propagating the prior reference frames and Gaussian noise through the Inflated 3D U-Net. For text conditioning, we employ FSText Composer to incorporate the text condition into the diffusion model.

With this design, Seer is able to generate high-quality, coherent and instruction-aligned videos by merely fine-tuning the autoregressive spatial-temporal attention layers and Frame Sequential Text Decomposer module. These two modules are jointly trained by the diffusion objective:

$$L_{\text{diffusion}} = \mathbb{E}_{t, \epsilon(\mathbf{x}), \mathbf{y}, \epsilon \sim \mathcal{N}(\mathbf{0}, \mathbf{I})} \left[ \|\epsilon - \epsilon_\theta(\mathbf{z}_t, t, f_\theta(\tau(\mathbf{y})))\|^2 \right], \quad (3)$$

where  $f_\theta$  is our FSText decomposer,  $\tau$  is the frozen CLIP text encoder, and  $\mathbf{y}$  is the input text.

### 4.2. Inflated 3D U-Net with Autoregressive Spatial-Temporal Attention

We inflate the Text-to-Image (T2I) pre-trained 2D U-Net to our Inflated 3D U-Net as illustrated in Figure 2 (b). A standard 2D U-Net block of LDMs consists of a series of 2D ResNet blocks and Spatial Attention Blocks including spatial self-attention and cross-attention modules. Similar to [12], we replace the  $3 \times 3$  2D convolution kernel with a  $1 \times 3 \times 3$  3D convolution kernel with an additional axis of video frames. Additionally, to further boost the performance of capturing the inter-frame dependency, we incorporate temporal attention after every spatial cross-attention layer. In Figure 3, we explore various types of temporal attention, including: (1) bi-directional temporal attention [12, 26, 9], which employs a full self-attention across all tokens along the temporal dimension; (2) directed temporal attention [43], which uses a masked attention mechanism that follows the direction of the video sequence along the temporal dimension; and (3) autoregressive spatial-temporal attention: a novel technique proposed by us, which uses causal attention to autoregressively generates the frames on both spatial and temporal dimensions by flattening the tokens into a long sequence.

We empirically observe that the two existing temporal attention layers cannot achieve promising performance on the TVP task. Bi-directional temporal attention tends to neglect the visual content guidance of the reference frames during the generation process (see Section 5.5). And the directed temporal attention fails to capture the dependency of nearby

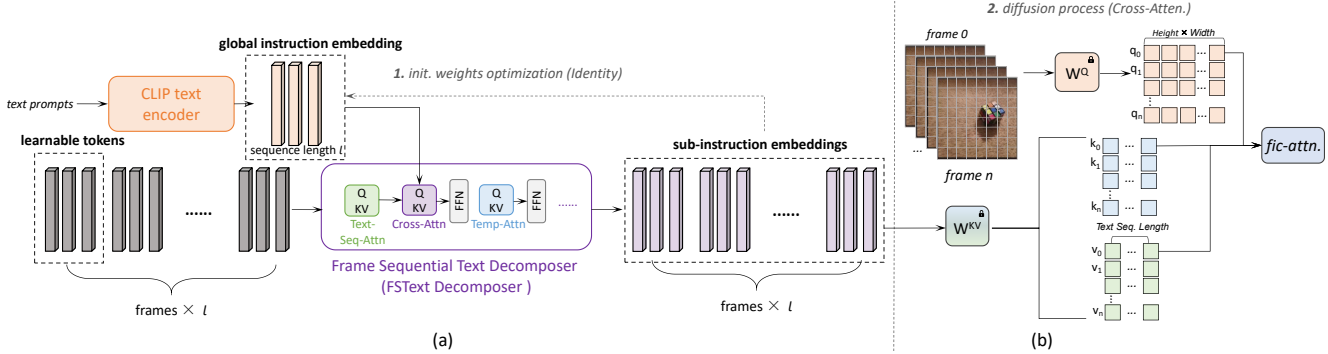


Figure 4: Frame Sequential Text Decomposer is shown in (a). We start by initializing the weight of the transformer network with learnable text tokens that are projected as identity vectors from CLIP text embeddings [18]. We then optimize the generated text tokens via the diffusion process (b), where frame-individual cross-attention is denoted by ‘‘fic-attn.’’

spatial regions and thus generates low-quality frames, while it adheres to the temporal sequence constraint.

To handle the limitations of bi-directional and directed temporal attention, we introduce the Autoregressive Spatial-Temporal Attention (AST-Attn) mechanism shown in Figure 3. Given  $n$  frames video, a video clip is projected into  $n \times s$  latent vectors (where  $s$  is the length of a latent vector in each frame) by the pre-trained VAE encoder. We flatten the latent vectors of both temporal and spatial dimensions ( $n \times s$ ) into one dimension. Then, AST-Attn performs self-attention on this long sequence with a causal mask that prevents the model from learning from future temporal-spatial tokens. Because it performs in both spatial and temporal spaces, the frame generation will attend to not only the previous frames but also the nearby spatial regions, which results in high-fidelity generation performance. While the calculation of Autoregressive Spatial-Temporal Attention (AST-Attn) involves both temporal and spatial dimensions, its computational complexity remains manageable due to the design of the Inflated 3D U-Net, which maintains the complexity of spatial compression rates and channel depths within a controllable range. Specifically, in the AST-Attn layers of Inflated 3D U-Net, higher-resolution features have more spatial tokens but are computed in lower embedding dimensions, while lower-resolution features have fewer spatial tokens but are computed in higher embedding dimensions. In practice, we observe that adopting AST-Attn has only a 0.4% computation speed lag compared to directed and bidirectional temporal attention.

By incorporating Autoregressive Spatial-Temporal Attention in the Inflated 3D U-Net, we can generate high-fidelity and coherent video frames with minimal fine-tuning. Specifically, we merely fine-tune the proposed autoregressive spatial-temporal attention layers and freeze the rest of the pre-trained layers in our Inflated 3D U-Net.

### 4.3. Frame Sequential Text Decomposer

For the language conditioning module, the existing methods [43, 26, 37] simply encode a single text embedding for the whole video with a CLIP text encoder [18]. However, the goals specified by the text instructions are usually in the task level, which makes it difficult for the model to figure out the progress at each timestep with a global instruction embedding. To better capture long-term dependency on both text and reference frames, we propose a Frame Sequential Text (FSText) Decomposer to decompose the global instruction into a sequence of fine-grained sub-instructions corresponding to each frame.

As illustrated in Figure 4, the FSText Decomposer takes in the global instruction embedding from CLIP text encoder [18] and decomposes them into sub-instructions for each timestep. Specifically, we introduce a sub-instruction embedding with  $l$  tokens for each frame, so there are  $n \times l$  learnable tokens in total, where  $n$  is the number of frames. At the start of the decomposer layer, learnable tokens learn the context dependency of the text by text sequential attention. Then, the global instruction embedding is decomposed into  $n$  timesteps by performing cross-attention with the  $n \times l$  learnable tokens. Through the projection of temporal attention and feedforward layers, learnable tokens obtain the fine-grained sub-instruction information, representing the progress of the macro-instruction being completed at each frame.

After getting  $n$  sub-instruction embeddings corresponding to each frame, the next step is to inject this guidance into the diffusion process, which is commonly completed by a cross-attention layer. As shown in Figure 4(b), different from the existing works that calculate the cross-attention between the global instruction embedding and  $n$  frames [12, 9, 43, 37], we propose to perform cross-attention individually between the visual latent vectors and sub-instruction embedding of each frame and then concat-

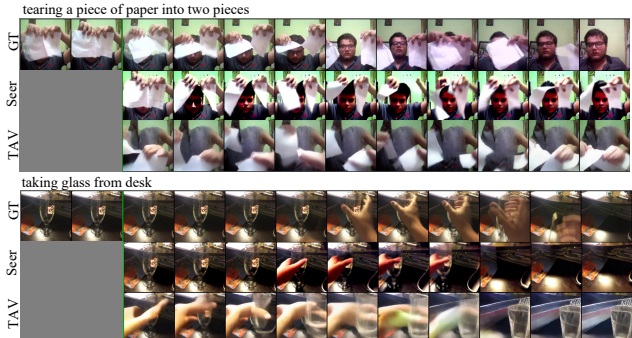


Figure 5: Visualization results of text-conditioned video prediction (conditioned on first 2 frames) on Something-Something V2. TAV refers to Tune-A-Video.

nate  $n$  results together, which is called Frame-individual Cross-Attention (*fic-attn*). Note that: the parameters in *fic-attn* are loaded from the T2I stable diffusion model and are frozen during training; and only the calculation of the attention scores for different frames is changed.

**Initialization** We find initialization is critical to FSText decomposer. Especially, the random initialization fails to approximate the distribution of text embeddings in the pre-trained T2I model and results in poor performance. To guarantee the sub-instruction embeddings become a close approximation of the CLIP text embedding, we employ an initialization strategy by enforcing the FSText decomposer to be an identity function. It can be achieved by this objective:

$$L_{\text{identity}} = \|f_{\theta}(\tau(\mathbf{y})) - \tau(\mathbf{y})\|^2 \quad (4)$$

Note that this initialization step is completed before the diffusion process. We will ablate this design in Section 5.5.

## 5. Experiments

In this section, we evaluate the proposed method Seer on the text-conditioned video prediction task. We compare against various recent methods and conduct ablation studies on the techniques presented in Section 4.

### 5.1. Datasets

We conduct experiments on two text-video datasets: Something Something-V2 (SSv2) [6], which contains videos of human behaviors involving everyday objects accompanied by language instructions, and BridgeData [3] that is rendered by a photo-realistic kitchen simulator with text prompts. Because the SSv2 validation set is too large (with over 200k samples), we follow [29] to evaluate the first 2048 samples during evaluation to save testing time. For BridgeData, we split the dataset into an 80% training set and 20% validation set, and evaluate all validation samples. To reduce complexity, we downsample each video clip to 12 frames for SSv2 and 16 frames for BridgeData during both training and evaluation. Moreover, to provide a fair

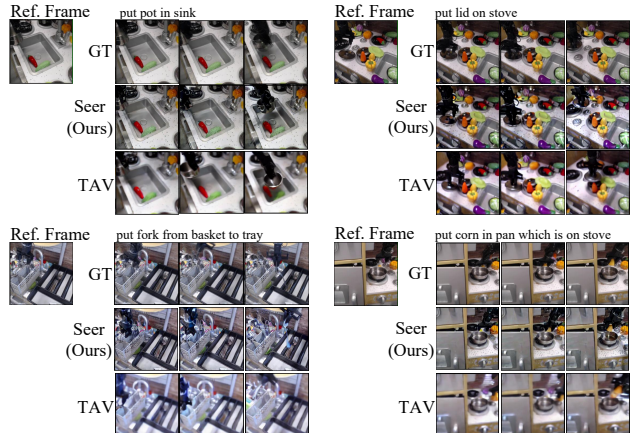


Figure 6: Visualization of Text-conditioned Video Prediction on Bridgedata. “Ref.” refers to reference frames and TAV refers to Tune-A-Video.

comparison with recent unreleased video generative model baselines [12, 8, 43, 26], we also included results on the UCF-101 dataset [29] in Appendix A.2.

### 5.2. Implementation Details

We use the pre-trained weights of the Tex-to-Image Latent Diffusion Model (LDM), Stable Diffusion-v1.5 [22], to initialize the VAE, ResNet Blocks and Spatial-Cross Attention layers of the 3D U-Net. We freeze both the pre-trained VAE and the pre-trained modules of the 3D U-Net, and only fine-tune the Autoregressive Spatial-Temporal Attention Layers. To fine-tune the FSText Decomposer, we initialized it as the identity function of the CLIP text embedding, as described in Section 4.3. We train the models on Something Something-V2 and BridgeData with an image resolution of  $256 \times 256$  for 20k training steps. In the evaluation stage, we speed up the sampling process with the fast sampler DDIM [27] and denoise the prediction with conditional guidance of 7.5 for 30 timesteps. Please refer to Appendix B for more details on hyperparameters.

### 5.3. Evaluation Settings

**Baselines.** We compare Seer with three publicly released baselines for video generation (1) conditional video diffusion methods: *Tune-A-Video* [37] and *Masked Conditional Video Diffusion* (MCVD)[34]; and (2) autoregressive-based transformer method: *Time-Agnostic VQGAN* and *Time-Sensitive Transformer* (TATS)[5]. Since Tune-A-Video is also the Text-to-Image inflated video diffusion model, and both MCVD and TATS are long video generative models for video prediction, they conform to our benchmark that requires predicting task-level movements. We further fine-tune Tune-A-Video, TATS, and train MCVD on the training sets of SSv2 and Bridgedata for 300k training steps.

**Machine Evaluation.** We evaluate the text-conditioned

Table 1: **Text-conditioned video prediction (TVP) results on Something-Something V2 (SSv2) and Bridgedata (Bridge).** We report the FVD and KVD metrics of each method. We can see that our method Seer achieves the lowest FVD and KVD values in both SSv2 and Bridgedata, illustrating our superior performance on the challenging TVP task.

Method	Pre-weight	Text	Resolution	SSv2 (ref. = 2)		Bridge (ref. = 1)	
				FVD↓	KVD↓	FVD↓	KVD↓
TATS [5]	video	No	128 × 128	428.1	2177	1253	6213
MCVD [34]	No	No	256 × 256	1407	3.80	1427	2.50
Tune-A-Video [37]	txt-img	Yes	256 × 256	291.4	0.91	515.7	2.01
Seer (Ours)	txt-img	Yes	256 × 256	<b>200.1</b>	<b>0.30</b>	<b>507.3</b>	<b>1.37</b>

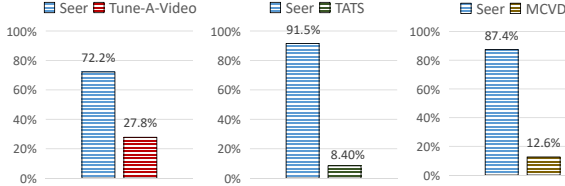


Figure 7: Human evaluation results. Preference percentage for text-conditioned video manipulation on SSv2.

video prediction of several baseline methods on Something Something-V2 (SSv2) (with 2 reference frames) and Bridgedata (with 1 reference frame). Additionally, we conduct several ablation studies of our proposed modules on SSv2. We report the Fréchet Video Distance (FVD) and Kernel Video Distance (KVD) metrics in our evaluation. FVD and KVD are calculated with the Kinetics-400 pre-trained I3D model [1]. We evaluate FVD and KVD on 2,048 SSv2 samples and 5,558 Bridgedata samples in the validation sets. For FVD metrics, we follow the evaluation code of VideoGPT [38]. We further evaluate the class-conditioned video prediction of our method on the UCF-101 dataset [29] and present the comparison results in Appendix A.2.

**Human Evaluation.** Besides evaluating the models on the standard validation sets, we also manually modify the text prompts to provide richer testing results, called text-conditioned video manipulation. Because of the absence of ground-truth frames, we conducted a human evaluation of text-conditioned video manipulation using 99 video clips from the validation set of SSv2. We manually modified partial text prompts and generated 99 predicted videos for each method. Then, we invited 54 anonymous evaluators to rate the quality of the prediction, with a higher priority placed on the semantic contents in the videos and an intermediate priority placed on the fidelity of the video frames. We report the percentage of overall preference choices among the 99 video clips. More details are introduced in Appendix D.

## 5.4. Main Results

**Quantitative Results.** Table 1 presents the text-conditioned video prediction results on Something Something-V2 (SSv2) and BridgeData. Seer achieves the best performance among all baselines, with the lowest Fréchet Video Distance (FVD) of 200.1 and Kinematic

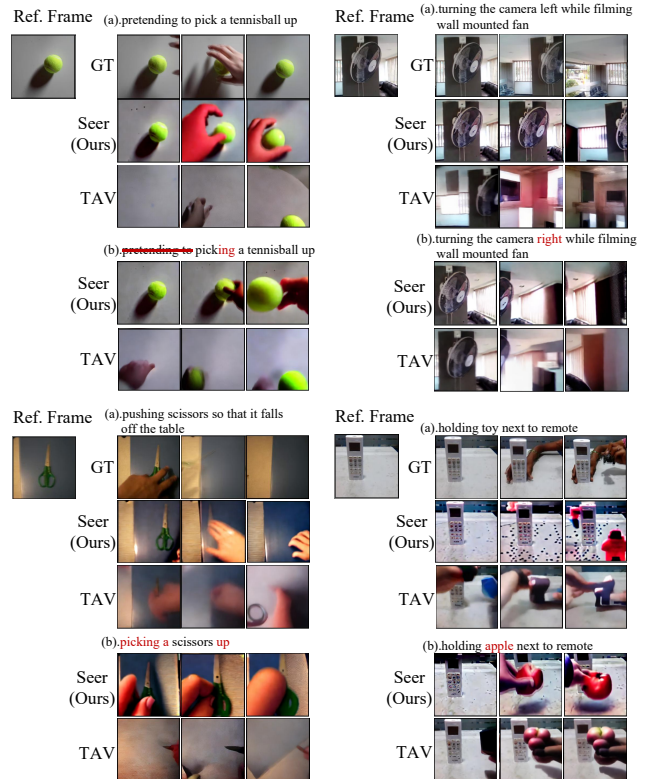


Figure 8: Visualization of Text-conditioned Video Prediction with the original (a) and manually modified (b) text prompts on Something-Something V2. “Ref.” is reference frames and TAV refers to Tune-A-Video.

Distance (KVD) of 0.3 in SSv2, and the lowest FVD of 507 and KVD of 1.37 in BridgeData. Notably, Seer and Tune-A-Video both incorporate text conditioning, and the results highlight Seer’s superior text-video alignment performance, especially on SSv2.

The results of the human evaluation in the text-conditioned video manipulation experiment are shown in Figure 7. Our proposed Seer outperforms the other baselines in terms of both semantic content and fidelity of video, with a preference rate of at least 72.2% in comparison. This indicates that Seer is effective in generating high-quality video clips that are faithful to the input text prompts.

**Qualitative Results.** Figure 5 compares the text-

Table 2: **Init. weight ablation results of FSText**

init. weight	FVD $\downarrow$	KVD $\downarrow$
random	367.9	0.75
identity(Ours)	200.1	0.30

Table 4: **Ablation study of Fine-tune settings**

fine-tune	FSText.	FVD $\downarrow$	KVD $\downarrow$
<i>temp-attn.</i>		328.2	1.26
<i>cross+temp-attn.</i>		249.9	0.73
<i>temp-attn.</i> (Ours)	✓	200.1	0.30
<i>cross+temp-attn.</i>	✓	1807	5.12

conditioned video prediction (TVP) performance of Seer and Tune-A-Video on Something Something-V2 (SSv2). While Tune-A-Video can align simple text prompts with video in some cases, it struggles to consistently track the spatial appearance of reference frames in later predictions. For instance, in the “taking glass from desk” samples, Tune-A-Video fails to generate a coherent motion trajectory and corrupts the pixels in the background, generating a new video instead of predicting from the reference frames. In contrast, Seer generates relatively coherent motion and better aligns the predictions with text prompts. Additionally, Seer can generate hidden objects by leveraging the imaging capability of the pretrained text-to-image diffusion model, which flexibly tackles occlusion issues in video prediction. In the “tearing a piece of paper into two pieces” sample, Seer accurately predicts that a man is hidden behind the paper and generates coherent frames including the man’s face. Figure 6 compares Seer and Tune-A-Video’s TVP performance on Bridgedata, illustrating that Seer achieves better text-video alignment, including the alignment of instructed behavior and target objects in future frames, and predicts a more coherent video with higher fidelity.

Figure 8 shows a comparison of Seer and Tune-A-Video for text-conditioned video prediction and manipulation on Something Something-V2 (SSv2). Tune-A-Video tends to mainly focus on Text-to-Video alignment, usually ignoring the directional temporal movement of the video. For example, in the case of “turning the camera left while filming wall mounted fan”, Tune-A-Video generates a semantic movement when the word “left” is replaced with “right” in the sentence, but fails to maintain temporal consistency in the video background during the transition from the middle to the last frame. In contrast, Seer performs better in handling the temporal dynamics of the video and achieving more precise text-video alignment in video manipulation.

### 5.5. Ablation study

In this section, we evaluate the effect of different components of our method in the TVP task on the SSv2 dataset.

**FSText Composer.** Table 2 compares different weight initialization strategies of FSText decomposer. The results

Table 3: **Ablation study of temporal attention**

temp. attn.	FVD $\downarrow$	KVD $\downarrow$
<i>bi-direct.</i>	258.2	0.56
<i>directed.</i>	222.3	0.40
<i>autoreg.</i> (Ours)	200.1	0.30

demonstrate that using identity initialization described in Section 4.3 yields higher prediction quality compared with random initialization. This finding demonstrates that identity initialization is necessary for the temporal-text projection of FSText decomposer. We also provide additional ablation results of FSText decomposer in Appendix A.4.

**Temporal Attention.** As shown in Table 3 studies the effectiveness of different types of temporal attention. Our autoregressive spatial-temporal attention (autoreg.) outperforms both bi-directional temporal attention (bi-direct.) and directed temporal attention (directed.), resulting in the lowest FVD and KVD scores. We also find that directed temporal attention further improves video prediction performance compared to bi-directional temporal attention because it utilizes the inductive bias of sequential generation.

**Fine-tune Setting.** We compare various fine-tuning settings of 3D Inflated U-Net, and the results are presented in Table 4. Our default setting involves fine-tuning both FSText decomposer (FSText.) and autoregressive spatial-temporal attention (AST-Attn.) layers (*temp-attn.*), while freezing the remaining modules in 3D U-Net. For the “*temp-attn.*” setting, we only finetune the AST-Attn. layers and freeze all other components. In the “*cross+temp-attn.*” setting, we jointly update the parameters of Spatial-Cross Attention layers and AST-Attn. layers. We further fine-tune the “*cross+temp-attn.*” together with FSText decomposer. We observe that our default setting achieves the highest quality of video prediction among all these settings, indicating that fine-tuning FSText decomposer is critical. Based on our default setting, further fine-tuning “*cross+temp-attn.*” causes the performance of Seer to drop a lot, even the worst among all fine-tuning settings. These results suggest that the optimization of the FSText decomposer is strongly guided by the frozen conditional diffusion prior, and additional fine-tuning of cross-attention leads to uncontrollable guidance to the FSText decomposer.

## 6. Conclusion

In this paper, we propose Seer, a sample and computation efficient model, for the challenging text-conditioned video prediction (TVP) task. We design autoregressive spatial-temporal attention (AST-Attn) and Frame Sequential Text (FSText) Decomposer to inflate the pretrained text-to-image (T2I) stable diffusion models along the temporal axis. With the rich prior knowledge contained in pretrained T2I models and the well-designed architecture, Seer successfully generates high-quality videos by only fine-tuning the AST-Attn and FSText Decomposer, which significantly reduces the data and computation costs. The experiments illustrate our superior performance over all the recent models.

## References

[1] Joao Carreira and Andrew Zisserman. Quo vadis, action recognition? a new model and the kinetics dataset. In *proceedings of the IEEE Conference on Computer Vision and Pattern Recognition*, pages 6299–6308, 2017. 7

[2] Ming Ding, Wendi Zheng, Wenyi Hong, and Jie Tang. Cogview2: Faster and better text-to-image generation via hierarchical transformers. In Alice H. Oh, Alekh Agarwal, Danielle Belgrave, and Kyunghyun Cho, editors, *Advances in Neural Information Processing Systems*, 2022. 3

[3] Frederik Ebert, Yanlai Yang, Karl Schmeckpeper, Bernadette Bucher, Georgios Georgakis, Kostas Daniilidis, Chelsea Finn, and Sergey Levine. Bridge data: Boosting generalization of robotic skills with cross-domain datasets. *arXiv preprint arXiv:2109.13396*, 2021. 2, 6

[4] Oran Gafni, Adam Polyak, Oron Ashual, Shelly Sheynin, Devi Parikh, and Yaniv Taigman. Make-a-scene: Scene-based text-to-image generation with human priors. In *Computer Vision–ECCV 2022: 17th European Conference, Tel Aviv, Israel, October 23–27, 2022, Proceedings, Part XV*, pages 89–106. Springer, 2022. 3

[5] Songwei Ge, Thomas Hayes, Harry Yang, Xi Yin, Guan Pang, David Jacobs, Jia-Bin Huang, and Devi Parikh. Long video generation with time-agnostic vqgan and time-sensitive transformer. In *Computer Vision–ECCV 2022: 17th European Conference, Tel Aviv, Israel, October 23–27, 2022, Proceedings, Part XVII*, pages 102–118. Springer, 2022. 2, 6, 7, 12

[6] Raghav Goyal, Samira Ebrahimi Kahou, Vincent Michalski, Joanna Materzynska, Susanne Westphal, Heuna Kim, Valentin Haenel, Ingo Fruend, Peter Yianilos, Moritz Mueller-Freitag, et al. The “something something” video database for learning and evaluating visual common sense. In *Proceedings of the IEEE international conference on computer vision*, pages 5842–5850, 2017. 2, 6

[7] Shuyang Gu, Dong Chen, Jianmin Bao, Fang Wen, Bo Zhang, Dongdong Chen, Lu Yuan, and Baining Guo. Vector quantized diffusion model for text-to-image synthesis. In *Proceedings of the IEEE/CVF Conference on Computer Vision and Pattern Recognition*, pages 10696–10706, 2022. 3

[8] Yingqing He, Tianyu Yang, Yong Zhang, Ying Shan, and Qifeng Chen. Latent video diffusion models for high-fidelity video generation with arbitrary lengths. *arXiv preprint arXiv:2211.13221*, 2022. 6, 12

[9] Jonathan Ho, William Chan, Chitwan Saharia, Jay Whang, Ruiqi Gao, Alexey Gritsenko, Diederik P Kingma, Ben Poole, Mohammad Norouzi, David J Fleet, et al. Imagen video: High definition video generation with diffusion models. *arXiv preprint arXiv:2210.02303*, 2022. 3, 4, 5

[10] Jonathan Ho, Ajay Jain, and Pieter Abbeel. Denoising diffusion probabilistic models. *Advances in Neural Information Processing Systems*, 33:6840–6851, 2020. 3

[11] Jonathan Ho and Tim Salimans. Classifier-free diffusion guidance. *arXiv preprint arXiv:2207.12598*, 2022. 3

[12] Jonathan Ho, Tim Salimans, Alexey Gritsenko, William Chan, Mohammad Norouzi, and David J Fleet. Video dif- fusion models. *arXiv preprint arXiv:2204.03458*, 2022. 1, 3, 4, 5, 6, 11, 12

[13] Wenyi Hong, Ming Ding, Wendi Zheng, Xinghan Liu, and Jie Tang. Cogvideo: Large-scale pretraining for text-to-video generation via transformers. In *International Conference on Learning Representations*, 2023. 1, 2, 3, 11, 12

[14] Tobias Höppe, Arash Mehrjou, Stefan Bauer, Didrik Nielsen, and Andrea Dittadi. Diffusion models for video prediction and infilling. *arXiv preprint arXiv:2206.07696*, 2022. 12

[15] Andrej Karpathy, George Toderici, Sanketh Shetty, Thomas Leung, Rahul Sukthankar, and Li Fei-Fei. Large-scale video classification with convolutional neural networks. In *Proceedings of the IEEE conference on Computer Vision and Pattern Recognition*, pages 1725–1732, 2014. 11

[16] Diederik P. Kingma and Max Welling. Auto-Encoding Variational Bayes. In *2nd International Conference on Learning Representations, ICLR 2014, Banff, AB, Canada, April 14–16, 2014, Conference Track Proceedings*, 2014. 3

[17] Alexander Quinn Nichol, Prafulla Dhariwal, Aditya Ramesh, Pranav Shyam, Pamela Mishkin, Bob McGrew, Ilya Sutskever, and Mark Chen. Glide: Towards photorealistic image generation and editing with text-guided diffusion models. In *International Conference on Machine Learning*, pages 16784–16804. PMLR, 2022. 3

[18] Alec Radford, Jong Wook Kim, Chris Hallacy, Aditya Ramesh, Gabriel Goh, Sandhini Agarwal, Girish Sastry, Amanda Askell, Pamela Mishkin, Jack Clark, et al. Learning transferable visual models from natural language supervision. In *International conference on machine learning*, pages 8748–8763. PMLR, 2021. 3, 5

[19] Aditya Ramesh, Prafulla Dhariwal, Alex Nichol, Casey Chu, and Mark Chen. Hierarchical text-conditional image generation with clip latents. *arXiv preprint arXiv:2204.06125*, 2022. 2, 3

[20] Aditya Ramesh, Mikhail Pavlov, Gabriel Goh, Scott Gray, Chelsea Voss, Alec Radford, Mark Chen, and Ilya Sutskever. Zero-shot text-to-image generation. In *International Conference on Machine Learning*, pages 8821–8831. PMLR, 2021. 3

[21] Scott Reed, Zeynep Akata, Xinchen Yan, Lajanugen Logeswaran, Bernt Schiele, and Honglak Lee. Generative adversarial text to image synthesis. In *International conference on machine learning*, pages 1060–1069. PMLR, 2016. 3

[22] Robin Rombach, Andreas Blattmann, Dominik Lorenz, Patrick Esser, and Björn Ommer. High-resolution image synthesis with latent diffusion models. In *Proceedings of the IEEE/CVF Conference on Computer Vision and Pattern Recognition*, pages 10684–10695, 2022. 2, 3, 4, 6

[23] Chitwan Saharia, William Chan, Saurabh Saxena, Lala Li, Jay Whang, Emily Denton, Seyed Kamyar Seyed Ghasemipour, Burcu Karagol Ayan, S Sara Mahdavi, Rapha Gontijo Lopes, et al. Photorealistic text-to-image diffusion models with deep language understanding. *arXiv preprint arXiv:2205.11487*, 2022. 3

[24] Masaki Saito, Shunta Saito, Masanori Koyama, and Sosuke Kobayashi. Train sparsely, generate densely: Memory-efficient unsupervised training of high-resolution temporal

gan. *International Journal of Computer Vision*, 128(10-11):2586–2606, 2020. 11, 12

[25] Christoph Schuhmann, Richard Vencu, Romain Beaumont, Robert Kaczmarezyk, Clayton Mullis, Aarush Katta, Theo Coombes, Jenia Jitsev, and Aran Komatsuzaki. Laion-400m: Open dataset of clip-filtered 400 million image-text pairs. *arXiv preprint arXiv:2111.02114*, 2021. 2

[26] Uriel Singer, Adam Polyak, Thomas Hayes, Xi Yin, Jie An, Songyang Zhang, Qiyuan Hu, Harry Yang, Oron Ashual, Oran Gafni, et al. Make-a-video: Text-to-video generation without text-video data. *arXiv preprint arXiv:2209.14792*, 2022. 1, 3, 4, 5, 6, 11, 12

[27] Jiaming Song, Chenlin Meng, and Stefano Ermon. Denoising diffusion implicit models. *arXiv preprint arXiv:2010.02502*, 2020. 6

[28] Yang Song, Jascha Sohl-Dickstein, Diederik P Kingma, Abhishek Kumar, Stefano Ermon, and Ben Poole. Score-based generative modeling through stochastic differential equations. In *International Conference on Learning Representations*, 2021. 3

[29] Khurram Soomro, Amir Roshan Zamir, and Mubarak Shah. Ucf101: A dataset of 101 human actions classes from videos in the wild. *arXiv preprint arXiv:1212.0402*, 2012. 6, 7, 11

[30] Du Tran, Lubomir Bourdev, Rob Fergus, Lorenzo Torresani, and Manohar Paluri. Learning spatiotemporal features with 3d convolutional networks. In *Proceedings of the IEEE international conference on computer vision*, pages 4489–4497, 2015. 11

[31] Sergey Tulyakov, Ming-Yu Liu, Xiaodong Yang, and Jan Kautz. Mocogan: Decomposing motion and content for video generation. In *Proceedings of the IEEE conference on computer vision and pattern recognition*, pages 1526–1535, 2018. 12

[32] Aaron Van Den Oord, Oriol Vinyals, et al. Neural discrete representation learning. *Advances in neural information processing systems*, 30, 2017. 3

[33] Ashish Vaswani, Noam Shazeer, Niki Parmar, Jakob Uszkoreit, Llion Jones, Aidan N Gomez, Łukasz Kaiser, and Illia Polosukhin. Attention is all you need. *Advances in neural information processing systems*, 30, 2017. 3

[34] Vikram Voleti, Alexia Jolicoeur-Martineau, and Christopher Pal. Masked conditional video diffusion for prediction, generation, and interpolation. *arXiv preprint arXiv:2205.09853*, 2022. 2, 6, 7, 12

[35] Chenfei Wu, Lun Huang, Qianxi Zhang, Binyang Li, Lei Ji, Fan Yang, Guillermo Sapiro, and Nan Duan. Godiva: Generating open-domain videos from natural descriptions. *arXiv preprint arXiv:2104.14806*, 2021. 1, 3

[36] Chenfei Wu, Jian Liang, Lei Ji, Fan Yang, Yuejian Fang, Dixin Jiang, and Nan Duan. Nüwa: Visual synthesis pre-training for neural visual world creation. In *Computer Vision–ECCV 2022: 17th European Conference, Tel Aviv, Israel, October 23–27, 2022, Proceedings, Part XVI*, pages 720–736. Springer, 2022. 1, 3

[37] Jay Zhangjie Wu, Yixiao Ge, Xintao Wang, Weixian Lei, Yuchao Gu, Wynne Hsu, Ying Shan, Xiaohu Qie, and Mike Zheng Shou. Tune-a-video: One-shot tuning of image diffusion models for text-to-video generation. *arXiv preprint arXiv:2212.11565*, 2022. 2, 3, 5, 6, 7

[38] Wilson Yan, Yunzhi Zhang, Pieter Abbeel, and Aravind Srinivas. Videogpt: Video generation using vq-vae and transformers. *arXiv preprint arXiv:2104.10157*, 2021. 7, 12

[39] Jiahui Yu, Yuanzhong Xu, Jing Yu Koh, Thang Luong, Gunjan Baid, Zirui Wang, Vijay Vasudevan, Alexander Ku, Yinfei Yang, Burcu Karagol Ayan, et al. Scaling autoregressive models for content-rich text-to-image generation. *arXiv preprint arXiv:2206.10789*, 2022. 3

[40] Lijun Yu, Yong Cheng, Kihyuk Sohn, José Lezama, Han Zhang, Huiwen Chang, Alexander G Hauptmann, Ming-Hsuan Yang, Yuan Hao, Irfan Essa, et al. Magvit: Masked generative video transformer. *arXiv preprint arXiv:2212.05199*, 2022. 12

[41] Sihyun Yu, Jihoon Tack, Sangwoo Mo, Hyunsu Kim, Junho Kim, Jung-Woo Ha, and Jinwoo Shin. Generating videos with dynamics-aware implicit generative adversarial networks. *arXiv preprint arXiv:2202.10571*, 2022. 12

[42] Daquan Zhou, Weimin Wang, Hanshu Yan, Weiwei Lv, Yizhe Zhu, and Jiashi Feng. Magicvideo: Efficient video generation with latent diffusion models. *arXiv preprint arXiv:2211.11018*, 2022. 2

[43] Daquan Zhou, Weimin Wang, Hanshu Yan, Weiwei Lv, Yizhe Zhu, and Jiashi Feng. Magicvideo: Efficient video generation with latent diffusion models. *arXiv preprint arXiv:2211.11018*, 2022. 3, 4, 5, 6, 11, 12

## A. Additional Experimental Results

### A.1. Implementation Details of Baselines

We compare three baselines in our paper. For Tune-A-Video, to ensure a fair comparison, we use the pre-trained weight of Stable Diffusion-v1.5<sup>1</sup> (same as our model) to initialize the UNet and we fine-tune the model with an image resolution of  $256 \times 256$  on the training sets of Something Something-V2 (SSv2) and Bridgedata for 200k training steps. For MCVD, we train the model with an image resolution of  $256 \times 256$  for 300k training steps. For TATS, we fine-tune the pre-trained UCF-101 model with an image resolution of  $128 \times 128$  on the training sets of SSv2 and Bridgedata for 300k training steps.

### A.2. Evaluation Details and Results of UCF-101

Most prior text-conditioned video generation methods [13, 12, 26, 43] evaluate their performance on the UCF-101 [29] benchmark. However, since our proposed method, Seer, is designed for text-conditioned video prediction (TVP) on task-level video datasets, the UCF-101 benchmark, which evaluates class-conditioned video prediction on random short-horizon video clips, is not an ideal evaluation benchmark for TVP. Nonetheless, in order to fairly compare these baselines, we still evaluate the class-conditioned video prediction performance of Seer on UCF-101.

**Settings** Specifically, we fine-tune our model with a video resolution of  $16 \times 256 \times 256$  on UCF-101. Following the evaluation protocols of [13], Seer predicts the videos conditioned on 5 reference frames during fine-tuning and inference stage. We report FVD and Inception score (IS) metrics on the UCF-101 dataset [29]. The IS is calculated by a C3D model[30] that is pre-trained on the Sports-1M dataset [15] and fine-tuned on UCF101. We follow the evaluation code of TGAN-v2 [24] to calculate IS metric. Following [13, 12, 26], we evaluate the FVD metric with 2,048 samples and IS metric with 100k samples in the validation set of UCF-101.

**Results** Table 5 presents the class-conditioned video prediction results on UCF-101, demonstrating that Seer outperforms CogVideo [13] and MagicVideo [43], but falls short of Make-A-Video [26]. Make-A-Video employs unlabelled video pre-training on temporal layers and achieves the best performance among all other methods. While Make-A-Video shows superior performance on FVD and IS, Seer has the potential to further improve its generation performance by addressing the following two limitations. First, Seer

<sup>1</sup><https://github.com/CompVis/stable-diffusion>

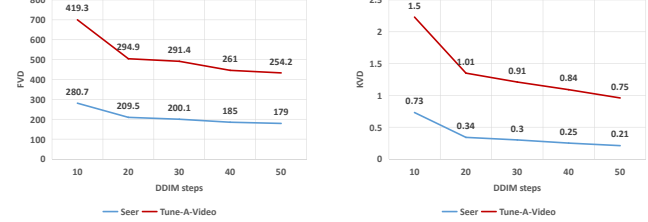


Figure 9: Evaluation results of Seer and Tune-A-Video with DDIM sampling steps ranging from 10 to 50 on the Something-Something V2 dataset.

has not been pre-trained on video data. Second, Seer obtains latent vectors via a pre-trained 2D VAE, which has not been fine-tuned on UCF-101 and limits the video generation quality of Seer (with 259.4 FVD and 68.16 IS reconstruction quality). However, as we focus on the text-conditioned video prediction task, addressing the above limitations on UCF-101 is out of the scope of this paper.

### A.3. Evaluation Results of Sampling Steps

To further investigate the generation effects of sampling steps during evaluation, we conduct a comparison between Seer and Tune-A-Video. We apply a series of DDIM sampling steps (10, 20, 30, 40, 50 DDIM steps), as shown in Figure 9. Seer consistently outperformed Tune-A-Video in terms of both FVD and KVD, with improvements observed from 20 DDIM steps to 50 DDIM steps. Particularly noteworthy is Seer’s advantage in video quality (280.7 FVD and 0.73 KVD) compared to Tune-A-Video (419.3 FVD and 1.5 KVD) when using only 10 DDIM steps, demonstrating Seer’s ability to sample high-fidelity videos efficiently with minimal denoising steps.

### A.4. Additional Ablation Results

**FSText layer depth** In this section, we additionally investigate the impact of FSText Decomposer’s layer depth in Table 6. Our default setting (8-layer FSText Decomposer) outperforms shallower models (2-layer and 4-layer) in terms of FVD. Though the 4-layer model shows a marginal advantage over the 8-layer model in terms of KVD, our experiments indicate that the 8-layer FSText Decomposer shows a remarkable advantage on FVD metrics and exhibits robustness in text-video alignment. Therefore, we adopt the 8-layer FSText Decomposer as the default setting for Seer.

**Qualitative results of fine-tuning ablation** We conduct a qualitative analysis of various fine-tune settings. We provide additional visualizations of Fine-tune Setting ablation in Section 5.5 of the main paper. Figure 10 shows the results of different settings. Among these settings, our default

Table 5: **Class-conditioned video prediction performance on UCF-101** we evaluate the Seer on the UCF-101 with 16-frames-long videos. Ex.data indicates that the model has been pre-trained or fine-tuned on extra datasets.

Method	Ex.data	Cond.	Resolution	FVD $\downarrow$	IS $\uparrow$
MoCoGAN-HD [31]	No	Class.	256 $\times$ 256	700 $\pm$ 24	33.95 $\pm$ 0.25
VideoGPT [38]	No	No	128 $\times$ 128	-	24.69 $\pm$ 0.30
RaMViD [14]	No	No	128 $\times$ 128	-	21.71 $\pm$ 0.21
StyleGAN-V [?]	No	No	128 $\times$ 128	-	23.94 $\pm$ 0.73
DIGAN [41]	No	No		577 $\pm$ 22	32.70 $\pm$ 0.35
TGANv2 [24]	No	Class.	128 $\times$ 128	1431.0	26.60 $\pm$ 0.47
VDM [12]	No	No	64 $\times$ 64	-	57.80 $\pm$ 1.3
TATS-base [5]	No	Class.	128 $\times$ 128	278 $\pm$ 11	79.28 $\pm$ 0.38
MCVD [34]	No	No	64 $\times$ 64	1143.0	-
LVDM [8]	No	No	256 $\times$ 256	372 $\pm$ 11	27 $\pm$ 1
MAGVIT-B [40]	No	Class.	128 $\times$ 128	159 $\pm$ 2	83.55 $\pm$ 0.14
CogVideo [13]	txt-img & txt-video	Class.	160 $\times$ 160	626	50.46
Make-A-Video [26]	txt-img & video	Class.	256 $\times$ 256	81.25	82.55
MagicVideo [43]	txt-img & txt-video	Class.		699	-
<b>Seer(Ours)</b>	txt-img	Class.	256 $\times$ 256	287.8	57.74
<b>pre-trained VAE*</b>	-	-	256 $\times$ 256	259.4	68.16

\* we evaluate the reconstruction quality of pre-trained 2D VAE in this table, the pre-trained 2D VAE is initialized with the pre-trained weight from Stable Diffusion-v1.5 without extra fine-tuning.

Table 6: **Layer depth in FSText Decomposer.**

num. layers.	FVD $\downarrow$	KVD $\downarrow$
2	238.6	0.51
4	229.7	0.23
8(Ours)	200.1	0.30

setting “*temp+FSText*” stands out as it preserves a higher-level temporal consistency in video prediction starting from reference frames and also delivers superior text-based video motion compared to the other fine-tune settings.

## B. Implementation Details

### B.1. Fine-tuning and Sampling

In this section, we list the hyperparameters, fine-tuning details, sampling details, and hardware information of our model in Table 7.

### B.2. Architecture information

In this section, we list the hyperparameters of 3D U-Net in Table 8 and hyperparameters of FSText Decomposer in Table 9.

## C. Visualization

### C.1. Additional qualitative results

We provide additional visualization on Something-Something v2 (SSv2) of our text-conditioned video prediction in Figure 11, and text-conditioned video prediction/manipulation results in Figure 12. Additionally, we

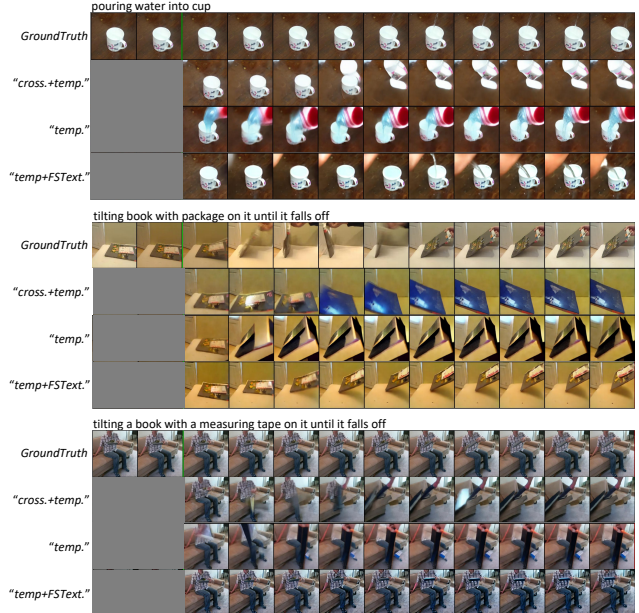


Figure 10: Additional qualitative results of fine-tuning ablation. “*temp+FSText.*” is our default setting.

provide the visualization on BridgeData of text-conditioned video prediction in Figure 13 and text-conditioned video prediction/manipulation in Figure 14.

## D. Human Evaluation Details

To evaluate the quality of video predictions according to human preferences, we conducted a human evaluation

Table 7: Hyperparameters and details of Fine Tuning/Inference

param.	value
optim.	AdamW
Adam- $\beta_1$	0.9
Adam- $\beta_2$	0.99
Adam- $\epsilon$	$1e^{-8}$
weight decay	$1e^{-2}$
lr	$1.28e^{-5}$
end lr	0.0
lr sche.	cosine
noise sche.	cosine
train batch size	1/GPU
grad. acc.	2
warmup steps	10k
resolution	$256 \times 256$
train. steps	200k
train. hardware	4 RTX 3090
val. batch size	2/GPU
sampler	DDIM
sampling steps	30
guidance scale	7.5

Table 8: Hyperparameters of 3D U-Net

hyperparam.	value
input/output channels	4
Base channels	320
Channel multipliers	1,2,4,4
3D Downsample blocks	4
3D Upsample blocks	4
Number of layers (per block)	2
Modules of layer	3D ResnetBlock Spatial-cross Atten. ATS Atten. Down./Up. 3D ResnetBlock
Dimension of atten. heads	8
activation function	SiLU
Dimension of cross-atten.	768

Table 9: Hyperparameters of FSText Decomposer

hyperparam.	value
learnable tokens channels	768
output channels	768
Base channels	768
Number of layers	8
Modules of layer	Seq-cross Atten. Feedforward Directed temporal Atten. Feedforward
Number of atten. heads	8
Dimension of cross-atten.	768

with 99 video clips on the validation set of the Something-Something V2 dataset (SSv2), the evaluation process involved 54 anonymous evaluators. To eliminate biases to

wards specific baselines, we randomly selected 20 questions for each evaluator. Each single-choice question consisted of a ground-truth video as a reference, a manually modified text instruction, and two video prediction results generated by Seer and another baseline method. The evaluators were required to choose the video clip that is more consistent with the text instruction and has higher fidelity from the two options. To ensure the clarity of the questions, we provided an example to explain the options in each questionnaire. Moreover, we recommended that evaluators prioritize video predictions with strong text-based motions as their first preference and the fidelity of the generated video as their second preference. For reference, Figure 15 provides a screenshot of an example questionnaire.

In total, we collected 342 responses for the Seer vs. TATS comparison, 363 responses for the Seer vs. Tune-A-Video comparison, and 357 responses for the Seer vs. MCVD comparison. And the results in the main paper Figure 7 are calculated based on the collected questionnaires.

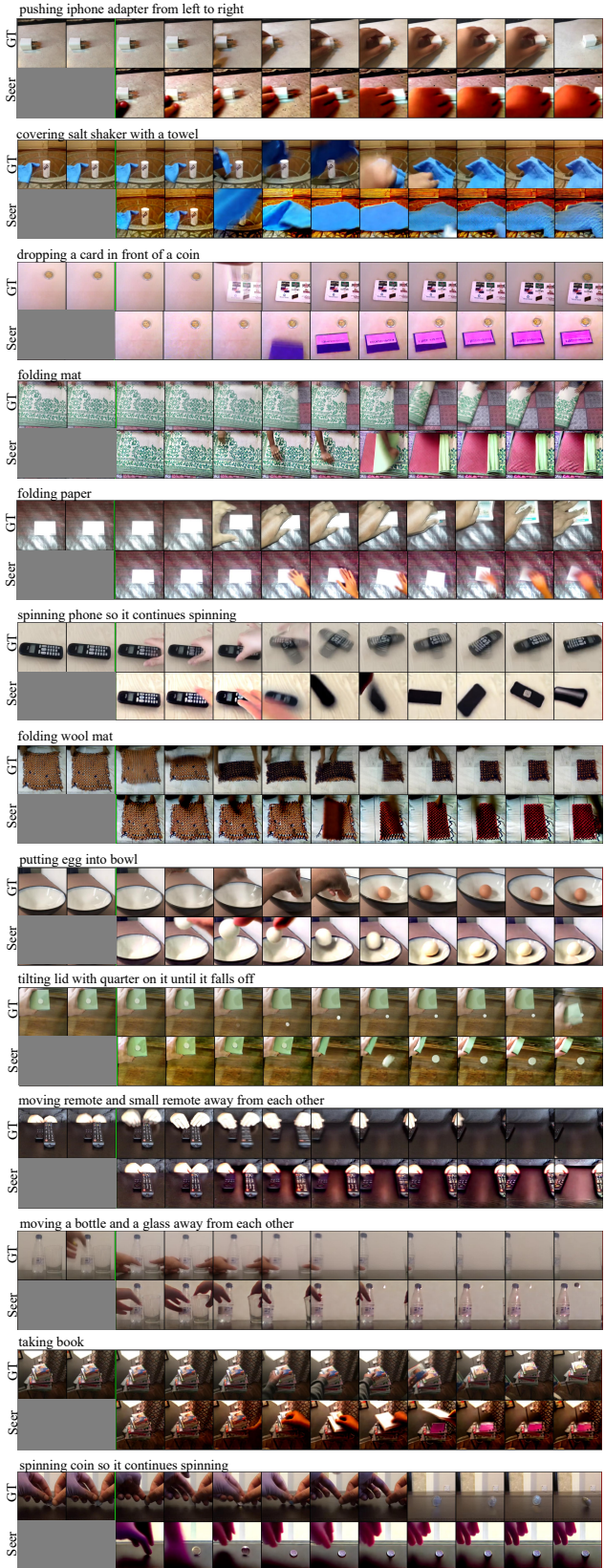


Figure 11: Text-conditioned video prediction of Seer on SSv2.

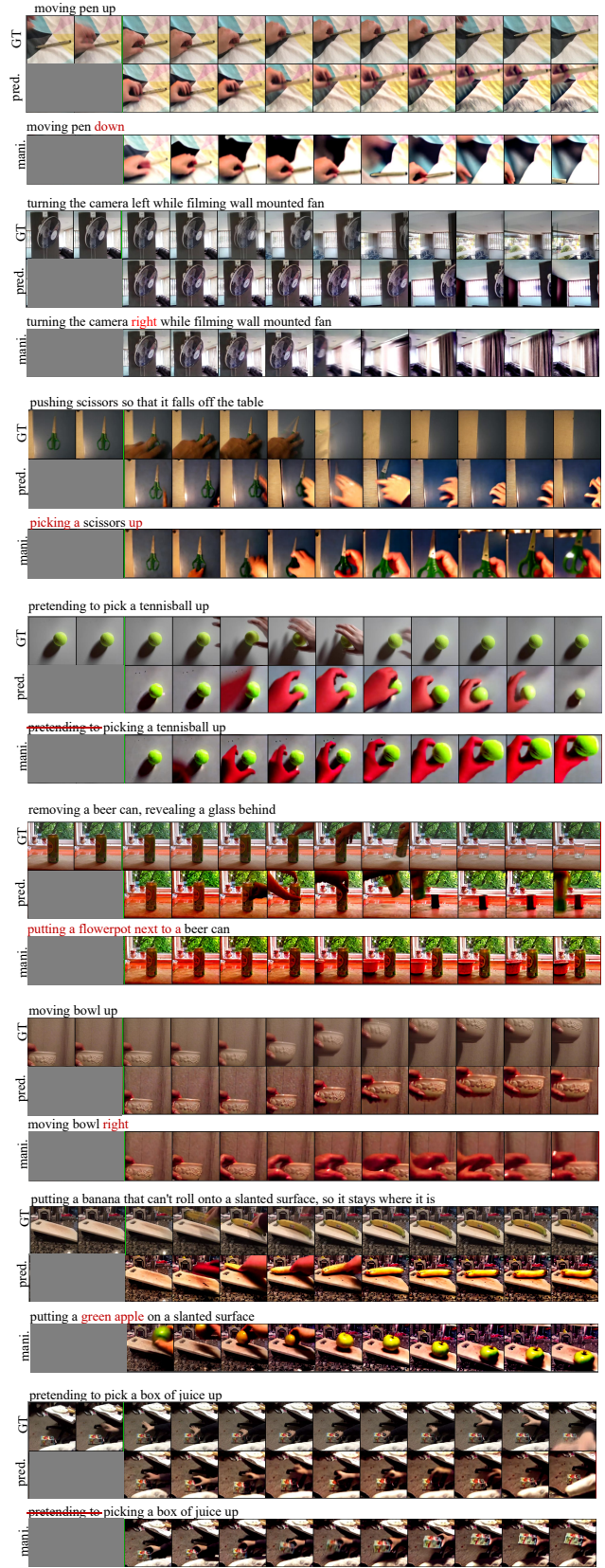


Figure 12: Text-conditioned video prediction/manipulation of Seer on SSv2, where “pred.” refers to prediction, “mani.” refers to manipulation.



Figure 13: Text-conditioned video prediction of Seer on BridgeData.



Figure 14: Text-conditioned video prediction/manipulation of Seer on BridgeData, where “pred.” refers to prediction, “mani.” refers to manipulation.

### Text-conditioned Video Prediction

Please review the text prompt and the reference video and choose the video result that is closer to the text description from the two options presented. If neither option accurately matches the text description, please choose the result that is more similar to the reference video, regardless of the resolution. For example, if the resolution is low but the generated result closely matches the text description, it is recommended to select that option.

**Example:**

According to the following text description, the video that needs to be generated is: "turning the camera right while filming wall-mounted fan". Please note that the given reference video may not match the language description exactly, but your task is to choose a video that accurately reflects the given language description.

Reference frame

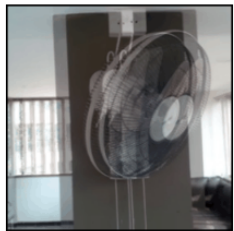


Figure 15: Screenshot of a questionnaire example shown to human evaluators.